

Wilson Goehe et al.
Supplemental Table 2

Cell line	Species and tissue of origin	Tumor Type	Phenotype
A549	Human lung	Adenocarcinoma	WT p53, K-ras ^{V12} mutation
H838	Human lung	Adenocarcinoma	p53 mutation, WT Ras
H2030	Human lung	Adenocarcinoma	WT p53, K-ras ^{V12} mutation
HBEC-3KT*	Human lung	N/A	WT p53, WT Ras

Characterization of cell lines utilized in Figure 1, Panels C and D with species, tissue of origin, tumor type, and phenotype. The HBEC-3KT* cell line has been immortalized by ectopic expression of cdk4 and hTERT30. WT = wild-type.

**Wilson Goehe et al.
Supplemental Table 3**

Cell line	Plasmid	Insert	Figure
A549	N/A	N/A	Figures 1-3,5-9
A549 Vector Control	pcDNA3.1(-)	N/A	Figures 2,3,6-9
A549 shRNA Control	TRC1/1.5 pKLO.1-puro	28mer scrambled shRNA	Figures 2 & 7
A549 Vector Control	pcDNA3	N/A	Figures 6,8 & 9
A549 + C9b ectopic	pcDNA3.1(-)	Caspase 9b cDNA	Figures 2 & 7
A549 + C9b shRNA	LentiMax	21mer C9b shRNA	Figure 2
A549 + hnRNP L shRNA	TRC1/1.5 pKLO.1-puro	21mer hnRNP L shRNA	Figures 6 & 7
A549 + hnRNP L ectopic	pcDNA3	hnRNP L cDNA	Figures 6,8 & 9

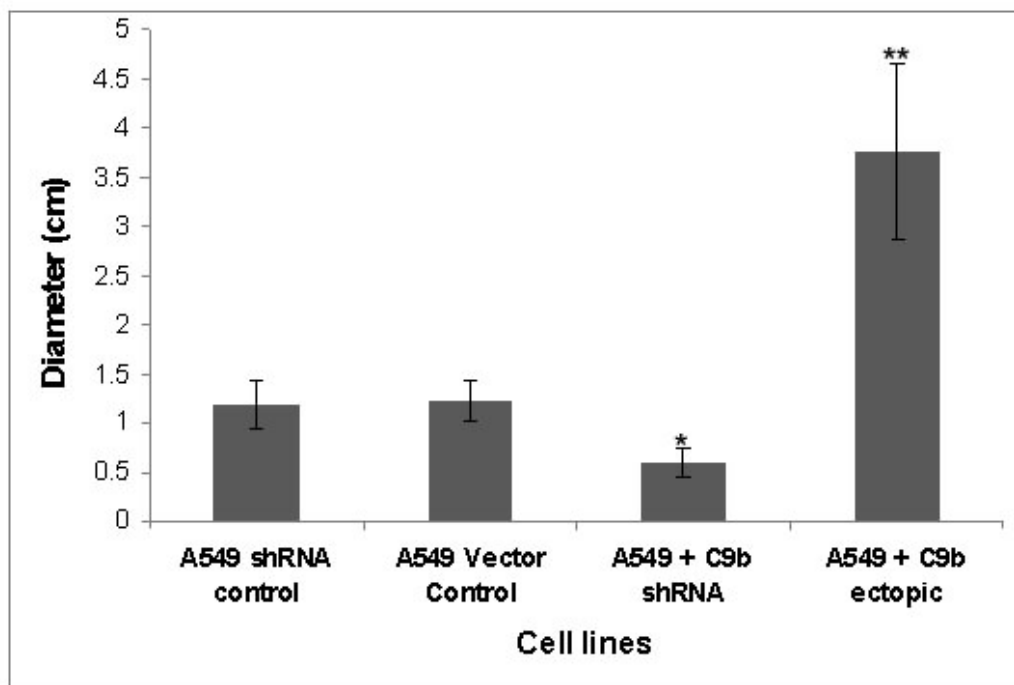
This table depicts multiple clones and "batch cultures" of A549 cells stably expressing the listed plasmids along with their appropriate insert. The figure(s) in which the cell lines were utilized is listed.

Wilson Goehe et al.
Supplemental Table 4

Possible phosphosite	Determination	ESI-LC-MS/MS confirmed	Affect on C9a/C9b ratio
Y47	Mass Spectrometry	Yes	No
Y48	Mass Spectrometry	Yes	No
Y92	Domain-motif prediction	No	No
Y363	Domain-motif prediction	No	No
S52	Mass Spectrometry	Yes	Yes
S250	Domain-motif prediction	No	No
S298	Mass Spectrometry	Yes	No
S381	Kinase site prediction	No	No
S542	Kinase site prediction	No	No
S543	Kinase site prediction	No	No
S544	Kinase site prediction	No	No
S553	Kinase site prediction	No	No
T98	Kinase site prediction	No	No
T577	Kinase site prediction	No	No

This table lists a range of possible phospho-sites for hnRNP L predicted by various phosphosite determination databases. Indicated are the specific residues, how the residues were determined, ESI-LC-MS/MS verified, and whether the residue demonstrated an effect on the caspase 9 splice variants.

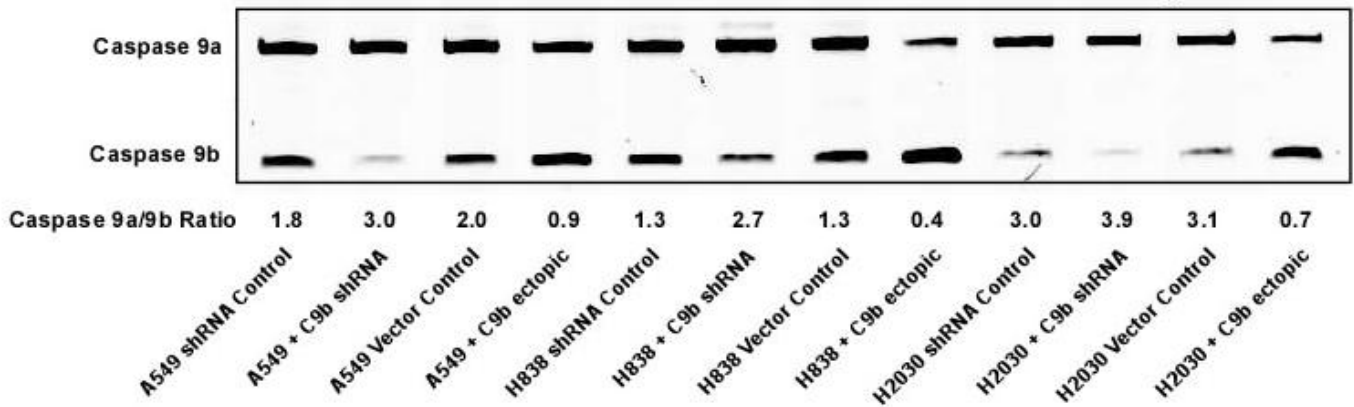
Wilson Goehe et al.
Supplemental Figure 1



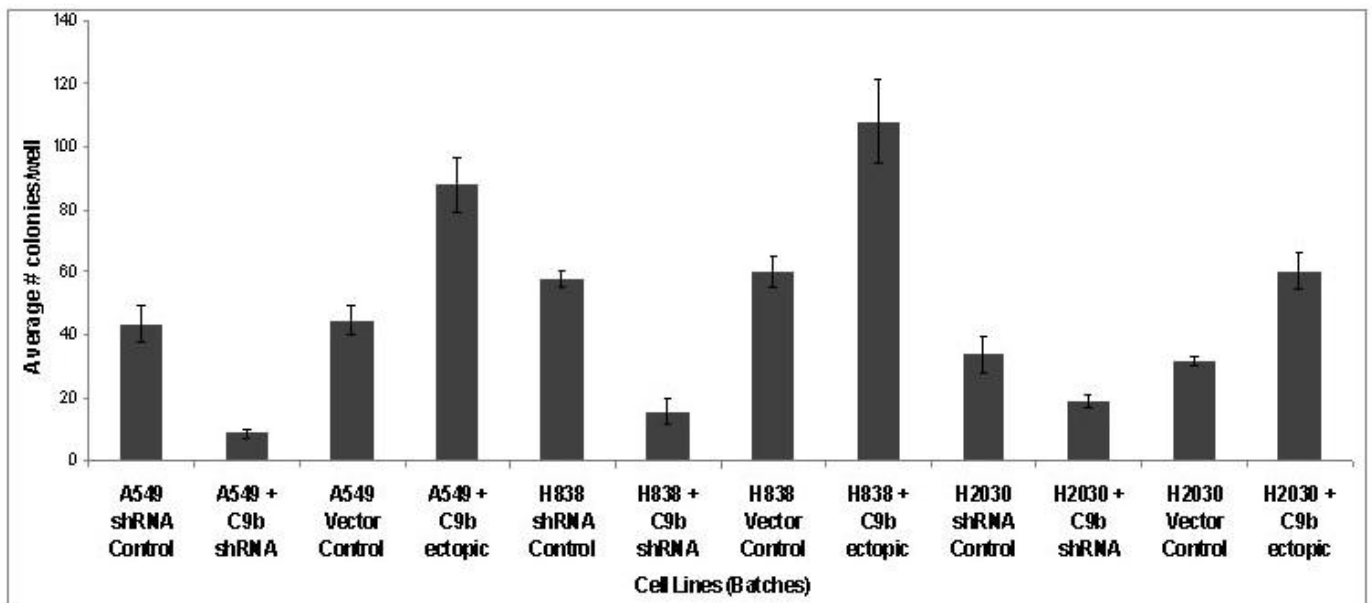
Supplemental Figure 1: Caspase 9b shRNA reduced the mean diameter of cellular colonies in anchorage-independent growth studies. Colony formation assays in soft agar for the A549 vector control, A549 + C9b shRNA, and A549 + C9b ectopic cell lines. A total of 2,000 cells were plated into 6-well tissue culture dishes in soft agar and cultured for 14 days before the colony count. Quantization (mean) of colony diameters (cm) for the indicated clonal cell lines. N=6; error bars represent SE; *P < 0.005 between A549 shRNA control versus A549 + hnRNP L shRNA, **P < 0.001 between A549 vector control versus A549 + C9b ectopic, student t-test.

Wilson Goehe et al.
Supplemental Figure 2

A

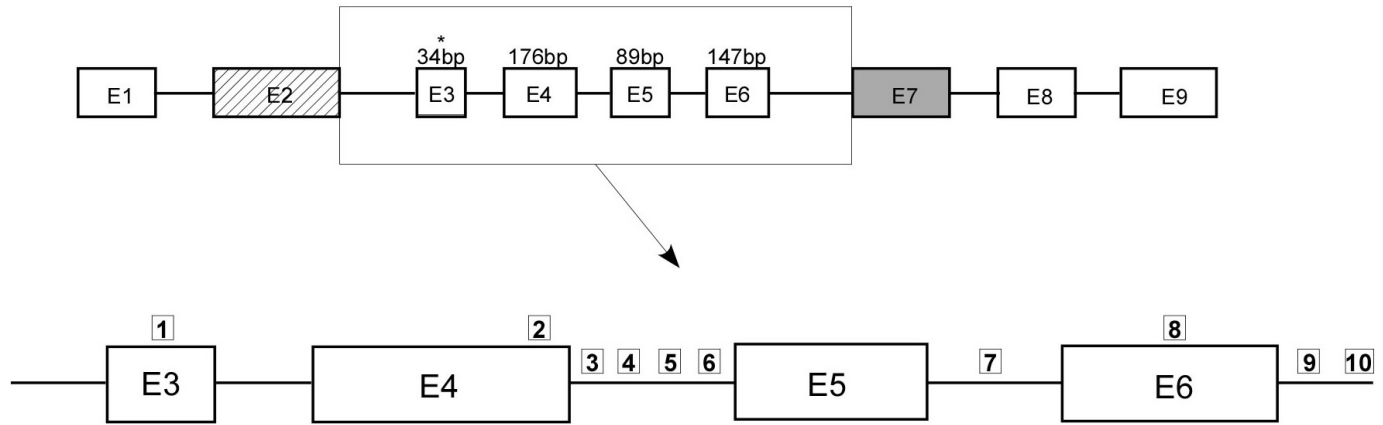


B



Supplemental Figure 2: A) Characterization of H838 and H2030s with caspase 9b shRNA or caspase 9b ectopic expression by quantitative/competitive RT-PCR analysis. **B)** Quantization of the number of colonies (% control) for H838 batch cell lines formed in soft agar. N=6; error bars represent SE.

**Wilson Goehe et al.
Supplemental Figure 3**

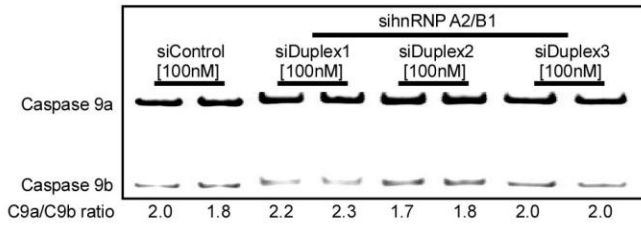


Number	Location	WT Sequence	Mutated Sequence
1	Exon 3	GAGAGTTT <u>GAGGGG</u> AAAT	GAGAGTTT <u>GCTACT</u> AAAT
2	Exon 4	T <u>GGTGG</u> AGGT	T <u>GCTCG</u> ACGT
3	Intron between E4-5	T <u>GGAGGG</u> AGAC	T <u>CGACGC</u> ACAC
4	Intron between E4-5	A <u>GGGTGGGGG</u>	A <u>CGCTCGCG</u>
5	Intron between E4-5	CAGT <u>GGGTGGGAAG</u>	CAGT <u>CGCTGCGCAAC</u>
6	Intron between E4-5	CAT <u>GGGAGG</u> TAGGAC	CAT <u>AAGCTTT</u> TAGGAC
7	Intron between E5-6	TGGGAGAG <u>GGGAGGG</u> GCAG	TGGGAGAA <u>AGCTTT</u> GCAG
8	Exon 6	CAGCCT <u>GGGAGGG</u>	CACCCT <u>CGCAGCG</u>
9	Intron between E6-7	T <u>GGGTGGGT</u>	T <u>CGCTGCGT</u>
10	Intron between E6-7	CT <u>GGTGGGGAGGGA</u>	CT <u>CGTCCAGCGA</u>

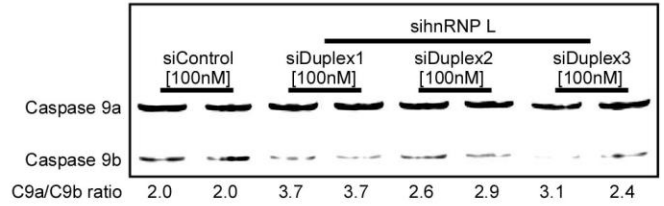
Supplemental Figure 3: Schematic representation of 10 potential regulatory *cis*-elements and their corresponding mutagenic sequences (No.'s 1-10) and location in caspase 9. Number 1 represents the sequence termed C9/E3-ESS.

Wilson Goehe at al.
Supplemental Figure 4

RT-PCR: Caspase 9



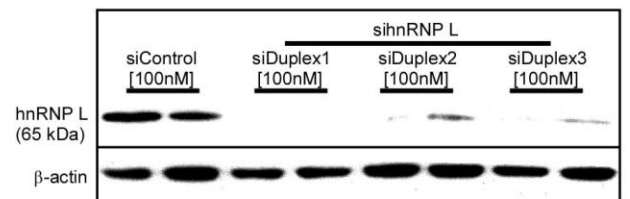
RT-PCR: Caspase 9



Western: hnRNP A2/B1

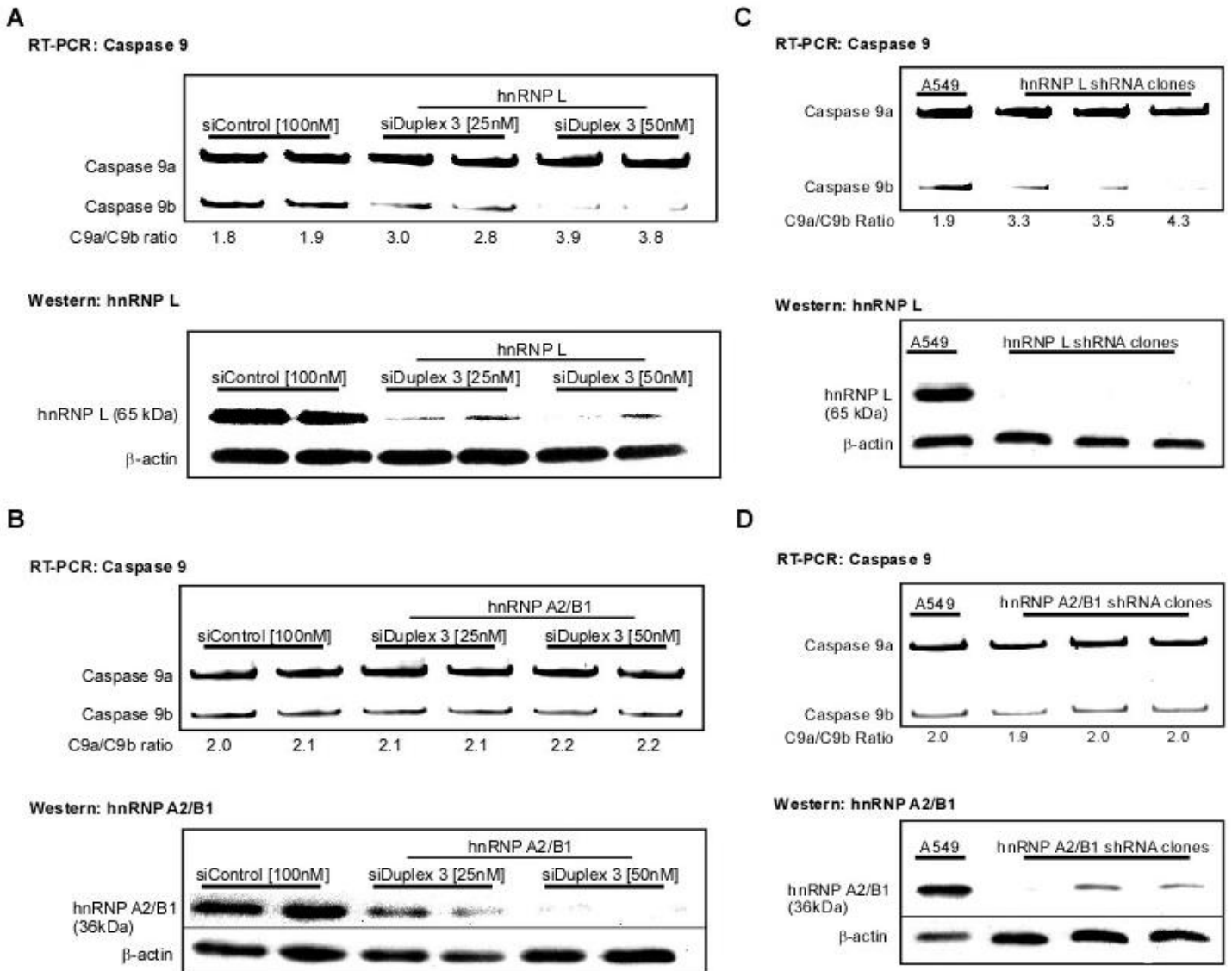


Western: hnRNP L



Supplemental Figure 4: A549 cells were transfected with 3 different duplex sequences of hnRNP L siRNA and hnRNP A2/B1 siRNA at a final concentration of 100 nM. As a control, scrambled siRNA (100 nM) was utilized. Total RNA was isolated and analyzed by competitive/quantitative RT-PCR for caspase 9 splice variants. The ratio of caspase 9a/9b mRNA was determined by densitometric analysis of RT-PCR fragments. Simultaneously, total protein lysates were also produced, subjected to SDS-PAGE analysis and immunoblotted for anti-hnRNP L, anti-hnRNP A2/B1, and β -actin as described in the “Materials and Methods” section. (A) hnRNP L; B) hnRNP A2/B1).

Wilson Goehe et al.
Supplemental Figure 5

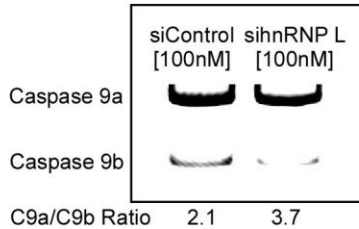


Supplemental Figure 5: A,B) A549 cells were transfected with a final concentration of 100nM control siRNA or dose-responsive treatments of 25 nM and 50 nM for sihnRNP L or sihnRNP A2/B1. Total RNA was isolated and analyzed by competitive/quantitative RT-PCR for caspase 9 splice variants. The ratio of caspase 9a/9b mRNA was determined by densitometric analysis of RT-PCR fragments. Simultaneously, total protein lysates were also produced, subjected to SDS-PAGE analysis and immunoblotted for hnRNP L, hnRNP A2/B1, and β -actin as described in the “Materials and Methods” section (A) hnRNP A2/B1; B) hnRNP L). Data represent 4 separate determinations on 3 separate occasions. **C,D)** Total RNA was isolated from A549 stable cell lines and analyzed by competitive/quantitative RT-PCR for caspase 9 splice variants. Total protein lysates were also produced, subjected to SDS-PAGE analysis and immunoblotted for hnRNP L, hnRNP A2/B1, and β -actin (C) hnRNP L; D) hnRNP A2/B1).

Wilson Goehe et al.
Supplemental Figure 6

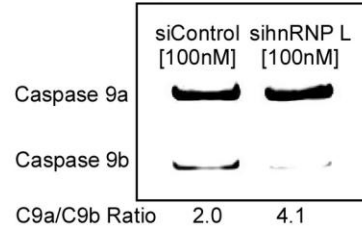
A H2030

RT-PCR: Caspase 9

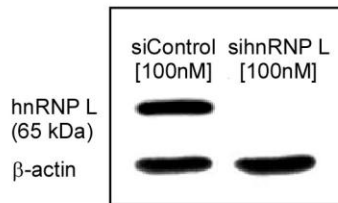


B H838

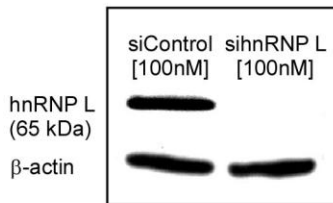
RT-PCR: Caspase 9



Western: hnRNP L



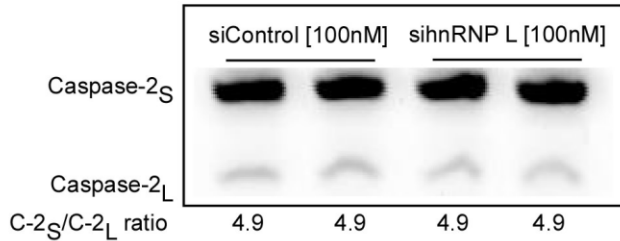
Western: hnRNP L



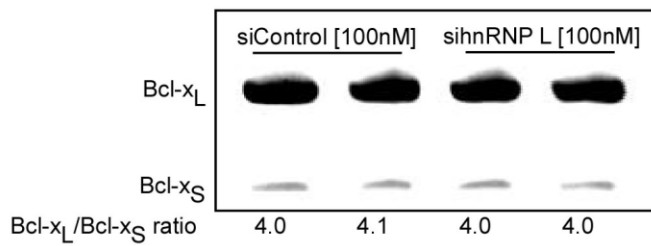
Supplemental Figure 6: H838 and H2030 cell lines were transfected with scrambled siRNA (100 nM), or hnRNP L SMARTpool siRNA (100 nM), for 48 hr. Total RNA was isolated and analyzed by competitive/quantitative RT-PCR for caspase 9 splice variants. The ratio of caspase 9a/9b mRNA was determined by densitometric analysis of RT-PCR fragments. Simultaneously, total protein lysates were also produced, subjected to SDS-PAGE analysis and immunoblotted for anti-hnRNP L and β -actin as described in the “Materials and Methods” section. Data are representative of three separate determinations on two separate occasions (A) H2030; B) H838).

Wilson Goehe et al.
Supplemental Figure 7

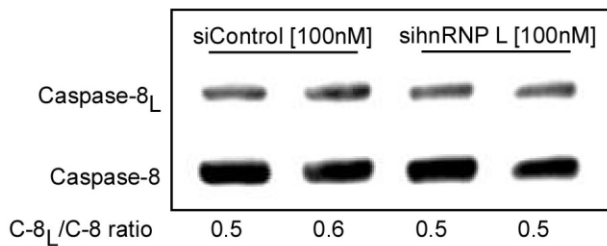
A Caspase 2



B Bcl-x

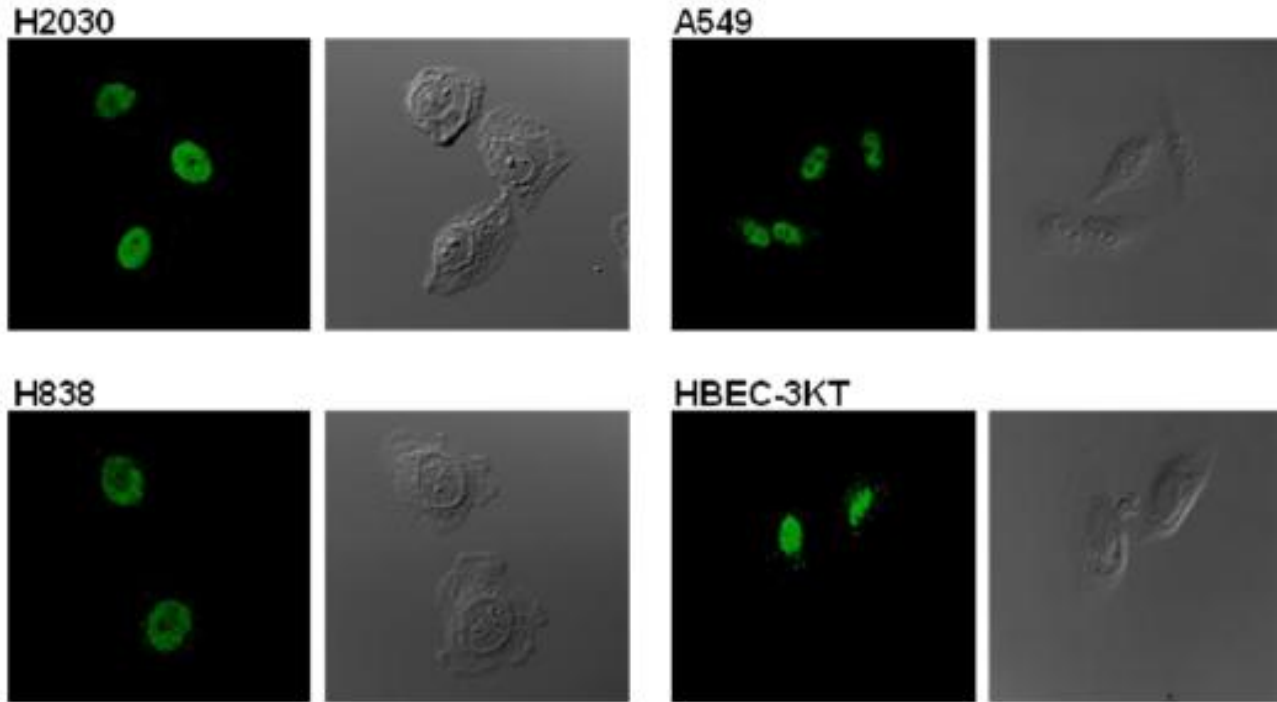


C Caspase 8



Supplemental Figure 7: A549 cells were transfected with scrambled siRNA (100 nM), or hnRNP L SMARTpool siRNA (100 nM) for 48 hr. Total RNA was isolated and analyzed by competitive/quantitative RT-PCR for the designated splice variants. The ratio of: A) caspase-2S/2L, B) Bcl-xL/Bcl-xS, and C) caspase-8L/caspase 8 mRNA was determined by densitometric analysis of RT-PCR fragments. Data are representative of three separate determinations on two separate occasions. Samples utilized for the presented data were verified to demonstrate significant effects on caspase 9 splicing in response to hnRNP L siRNA.

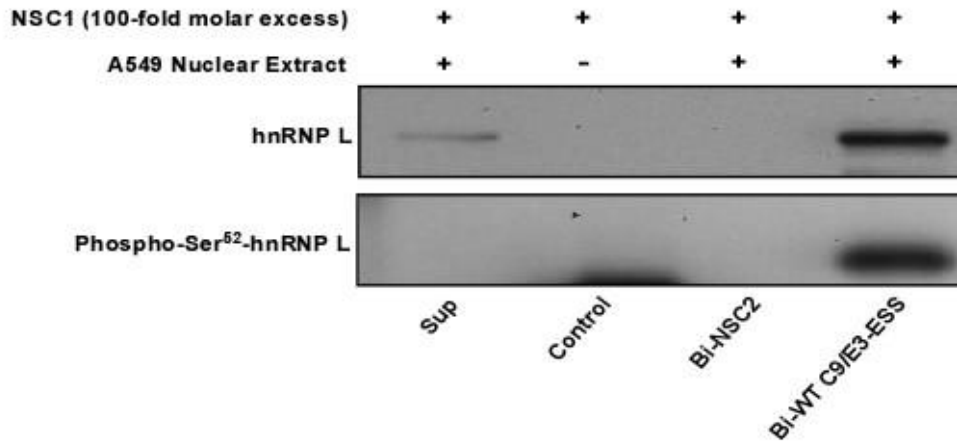
Wilson Goehe et al.
Supplemental Figure 8



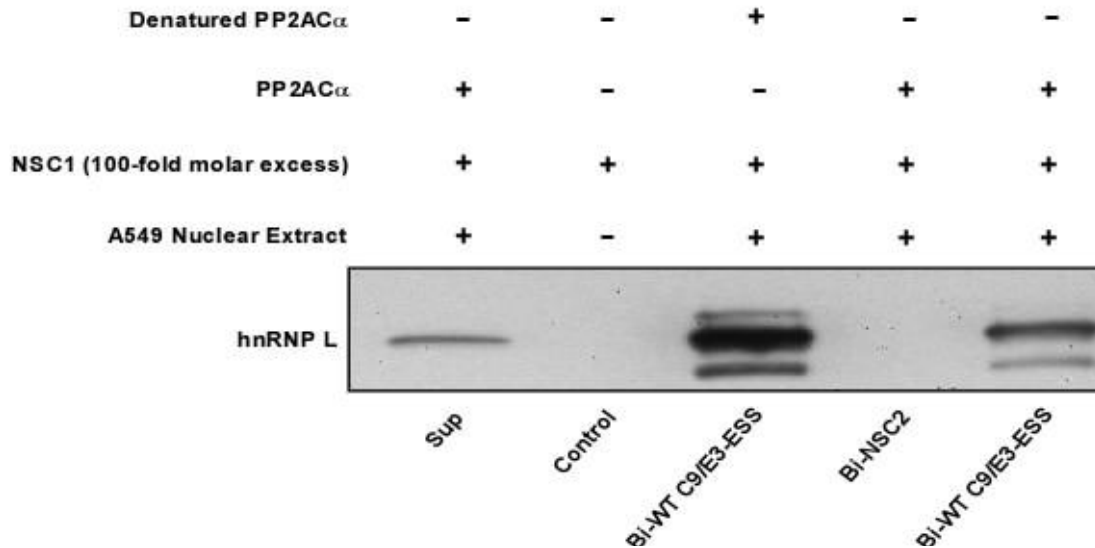
Supplemental Figure 8: For confocal microscopy, the A549, H838, H2030, and HBEC-3KT cell lines (5×10^3) were seeded onto coverslips and subjected to standard incubator conditions for 24 hrs. Cells were then fixed with 100% cold methanol for 10 min at -20°C . The slides were washed extensively after fixing with PBS containing 10 mM glycine and 0.2% sodium azide. The cells were then incubated for 1 hr with the primary antibody, hnRNP L (1:100), followed by incubation with an AlexaFlour488 anti-mouse secondary antibody (1:500) (green).

Wilson Goehe et al.
Supplemental Figure 9

A

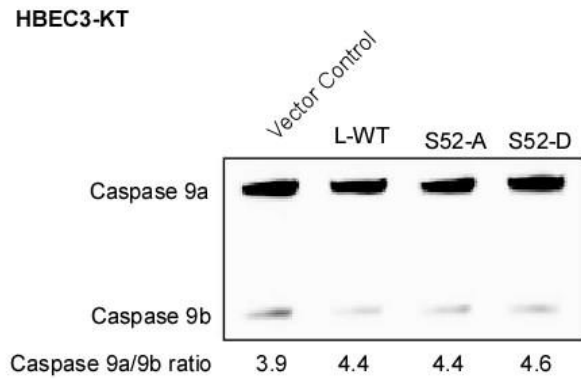


B



Supplemental Figure 9: Phospho-Ser⁵²-hnRNP L binds specifically to the exonic splicing silencer in exon 3 of caspase 9. **A)** A 5' biotinylated wild-type C9/E3-ESS RO (Bio-C9/E3-ESS) or 5'biotinylated non-specific RO (Bio-NSC-2) were incubated in the presence of nuclear extract from A549 cells or IgG (control), subjected to SDS-PAGE and western immunoblotting analysis (anti-hnRNP L; anti-Phospho-Ser⁵²-hnRNP L). An unlabeled non-specific RO (e.g NSC-1) at a 100-fold excess were also added to the reactions as indicated. Sup designates the corresponding supernatant from the Bio-WT C9/E3-ESS to show the remaining RNA *trans*-factor after affinity purification. **B)** The Panel A experiment was repeated but with the addition of either denatured PP2AC α or denatured PP2AC α as indicated.

Wilson Goehe et al.
Supplemental Figure 10



Supplemental Figure 10: HBEC3-KT cells were transfected with either wild-type hnRNP L (WT-hnRNP L) (0.25 μ g), Ser⁵²Ala hnRNP L (S52-A) (0.25 μ g), or Ser⁵²Asp hnRNP L (S52-D) (0.25 μ g) for 24 hrs. Total RNA was extracted and analyzed by competitive/quantitative RT-PCR for caspase 9 splice variants. Data are N=3 from 3 separate occasions.